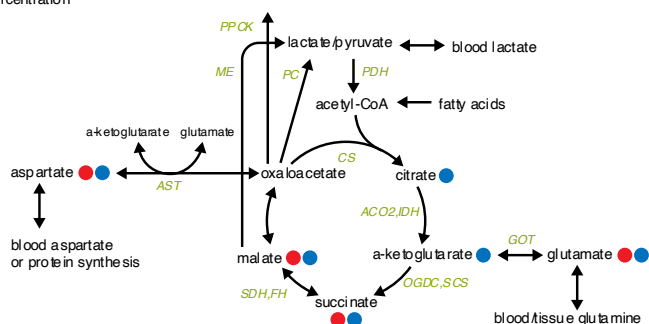


Supplementary Note 1: TCA flux inference by non-stationary metabolic flux analysis

To infer tissue specific TCA turning, anaplerotic, and anabolic fluxes we developed an isotopomer model that describes how labeled substrates propagate through the TCA cycle reactions in a non-stationary manner^{1,2}. This TCA labeling model is derived from a reaction network of the TCA cycle accounting for TCA cycle reactions, malic enzyme, pyruvate carboxylase, phosphoenolpyruvate carboxykinase, as well as the aspartate and glutamate transaminases. The model further considers that labeling from the circulation (from infused [U-¹³C] lactate or [U-¹³C] glutamine tracer) is diluted by tissue production of lactate/pyruvate from unlabeled glucose, two-carbon contributions from fatty-acid β -oxidation and five-carbon contributions via glutamine/glutamate. We construct the model around metabolite mass balances for a combined tissue lactate/pyruvate pool (pyr), acetyl-CoA (accoa), citrate/isocitrate (cit), α -ketoglutarate (akg), glutamate (glu), succinate (succ), malate (mal), oxaloacetate (oaa) and aspartate (asp) resulting from the reaction network presented in Figure S1. We further assume that all reactions operate far from equilibrium except for fumarase, succinate dehydrogenase, malate dehydrogenase, and the transaminases (AST, GOT).

model inputs:

- labeling time points from [U-¹³C] lactate or glutamine
- concentration



reduced model parameters:

- | | |
|------------|---|
| V_{TCA} | TCA (Citrate synthase) flux |
| V_{ME} | Malic enzyme flux |
| V_{PPCK} | Phosphoenolpyruvate carboxykinase flux |
| d_l | blood lactate contribution to tissue pyruvate |
| d_a | pyruvate contribution to acetyl-CoA |
| d_g | blood glutamine contribution to α -ketoglutarate |
| r | Fraction of tissue pyruvate consumed by PDH |
| R_r | Flux reversibilities for all reversible transformations |

Figure S1: TCA model and parameters. PC: pyruvate carboxylase, PDH pyruvate dehydrogenase, CS citrate synthase, ACO2 aconitase, IDH isocitrate dehydrogenase, GOT glutamate transaminases, OGDC oxoglutarate dehydrogenase complex, SCS succinate synthase, SDH succinate dehydrogenase, FH fumarase, MDH malate dehydrogenase, PPCK phosphoenolpyruvate carboxykinase, AST aspartate aminotransferase, ME malic enzyme, EXLAC blood lactate exchange, EXGLN blood glutamine exchange, EXFA Fatty Acid exchange, EXASP aspartate exchange.

From this reaction network and its associated carbon atom mappings (see Table S1), we then compute all possible isotopomers that can be produced from a specific tracer, such as [U-¹³C] lactate or [U-¹³C] glutamine. For computational efficiency, condensation reactions between labeled substrates are omitted, since the mean labeling of isotopic forms is 3% (max 11%), making the typical condensation product too rare to merit consideration, i.e. typical fraction of $(3\%)^2 < 0.1\%$ (see Table S1). Moreover, for several tested tissues, modeling including all condensation reactions and associated isotopic forms yielded indistinguishable fluxes from those obtained with omission of these minor species (Extended Data Figure 3D).

The list of possible isotopomers connected by the reactions in the above presented network allows us then to construct a model describing the time evolution of the labeled isotopomer

compounds as an ordinary differential equation (ODE)^{1,2}. This model is derived from the individual mass balances of the isotopomer concentrations K :

$$\frac{dK}{dt} = Nf \quad (1)$$

where f_j are isotopomer-specific transition rates and N is a matrix describing the isotopomer specific stoichiometry: for example, one such transition is the transition from α -ketoglutarate 00011, with carbon-13 atoms in the 4 and 5 positions, to succinate 1100 with carbon-13 atoms in the 1 and 2 positions. It is convenient to express the isotopomer concentrations in terms of their pool sizes, i.e. the concentration of the parent metabolite p (which includes all possible isotopomers), and the respective isotopomer enrichments L_k :

$$K = XL \quad (2)$$

where X is a diagonal matrix containing the total pool size $[X_p]$ associated with the respective isotopomer labeling fraction L_i . Similarly, we can express the isotopomer specific transition rates in terms of the labeling fractions of the products and the fluxes of the respective biochemical reaction r as:

$$f_j = v_r \prod_{k=1}^{N_I} L_k^{n_{kj}^-} \quad (3)$$

where v_r is the flux of the reaction r associated with the isotopomer transition j , and n_{kj}^- is the positimized substrate stoichiometry:

$$n_{kj}^- = \begin{cases} |n_{kj}| & n_{kj} < 0 \\ 0 & \text{elsewhere} \end{cases} \quad (4)$$

Since the infusions are minimally perturbative (Extended Data Figure 1D), we can consider the system (except for isotopes/isotopomers) to be at approximate steady-state throughout the infusion period:

$$\frac{dX}{dt} = Sv \approx 0 \quad (5)$$

where $X = [pyr], [accoa], [cit], [akg], [glu], [succ], [mal], [oaa]$, contains the pool concentrations, S is the stoichiometric matrix, and v is a vector of fluxes for the reactions denoted in S . We can then rewrite Eq. 1 as:

$$X \frac{dL}{dt} = Nf(L, v) \quad (6)$$

Thus, describing the non-stationary propagation of the carbon label through the network N reduces to finding a set of fluxes v that are able to explain time dependency of the labeling of the m+1,2,3 isotopic forms. Since we consider the system to operate at steady state, these fluxes are not independent from one another.

We express the dilution effects from lactate, fatty acids and glutamine as fractional flux contributions: d_l is circulating lactate contribution to the tissue pyruvate production; d_p is tissue

pyruvate contribution to tissue acetyl-CoA production; d_g is blood glutamine contribution to tissue glutamate production and r is the fraction of pyruvate consumed by pyruvate dehydrogenase (while the remainder is consumed by pyruvate carboxylase). These parameters allow us to reformulate the model in terms of three free fluxes: i) TCA turning flux v_{TCA} , ii) malic enzyme flux v_{ME} , and iii) phosphoenolpyruvate carboxykinase flux (i.e. gluconeogenic flux) v_{PPCK} . All the other fluxes of the model can be back-calculated from the mass balance constraints. (For derived expressions see Table S2).

Furthermore, we reformulate the forward v_r^F and reverse flux v_r^R of the reversible reactions in terms of the respective net flux that is constrained by the overall mass balance and a dimensionless reversibility R_r that approaches $R_r \rightarrow 1$ for the case that the reaction operates far from equilibrium and $R_r \rightarrow \infty$ for the case that the reaction is close to equilibrium:

$$R_r = \frac{v_r^f + v_r^R}{|v_r^f - v_r^R|} = \frac{v_r^f + v_r^R}{|v_r|} \quad (7)$$

This results in a reduced model that requires us to identify 14 parameters: three free fluxes $\{v_{TCA}, v_{ME}, v_{PPCK}\} \in \mathbb{R}^+$, four dimensionless flux contributions $\{d_l, d_p, d_g, r\} \in [0,1]$, as well as seven dimensionless reversibilities $\{R_{lac,in}, R_{glu,in}, R_{asp,in}, R_{MDH}, R_{TAG}, R_{AACT}, R_{SDH,FB}\} \in [1, \infty)$.

We then find 14 parameters that best explain the observed labeling dynamics by minimizing least-square residuals between the measured and simulated time-dependent isotope enrichments for a fixed set of metabolite concentrations (selected based on the experimental measurements of those concentrations and their error, see below). We simulate these labeling patterns by solving the initial value problem for Equation 6, assuming that at $t = 0$ all isotope-labeled fractions L_k are zero (as these reflect the measured labeling *after* correction for natural isotope abundance). The output of the simulation provides us with the labeling dynamics of all the isotopomers for a given set of parameters (fluxes, reversibilities, and flux contributions). We then calculate the residuals of the time-dependent cumulative labeling from the isotope-labeled forms containing m+1,2,3 carbon-13-labeled atoms using the experimental data, i.e. tissue glutamate, malate, aspartate, and succinate resulting from tissue sampling at different timepoints after primed tracer infusion, as well as arterial blood labeling of tracer metabolite (i.e. lactate or glutamine). We solve the resulting least-square optimization problem using the Levenberg–Marquardt algorithm^{3,4}.

To find a global optimum under the uncertainty of the pool size measurements X we initialize 2000 initial guesses with the pool sizes sampled from a normal distribution following the experimental observations of the pool size concentrations, i.e. tissue concentrations of glutamate, malate, aspartate, succinate, α -ketoglutarate, and citrate/isocitrate, and uniformly distributed initial parameter guesses. To determine the error of the flux estimate we solve the optimization problem with different initial guesses and tissue concentrations drawn from a normal distribution. Subsequently we estimate the median flux and its 95% confidence interval by bootstrapping: we randomly resample the best 20 fits from 2000 parameter estimates 100 times

Table S1: Atom mapping for the reactions of the reduced TCA model.

Reaction	Symetric	Substrates	Products
PDH	no	pyr (abc)	accoa (bc)
CS	no	accoa (ab) , oaa (cdef)	cit (fedbac)
ACO2/IDH	no	cit (abcdef)	akg (abcde)
GOT (F)	no	akg (abcde)	glu (abcde)
GOT (R)	no	glu (abcde)	akg (abcde)
OGDC/SCS	no	akg (abcde)	succ (bcde)
SDH/Fh (F)	yes	succ (abcd)	mal (abcd)
SDH/Fh (R)	yes	mal (abcd)	succ (abcd)
MDH	no	mal (abcd)	oaa (abcd)
PC	no	pyr (bcd),	oaa (abcd)
ME	no	mal (abcd)	pyr (bcd)
AST (F)	no	oaa (abcd) + glu (efghi)	asp (abcd) + akg (efghi)
AST (R)	no	asp (abcd) + akg (efghi)	oaa (abcd) + glu (efghi)

Table S2: Expressions relating reaction rate to model variables

Reaction	Symbol	Type	Expression
PDH	v_{PDH}	dependent	$v_{TCA}d_a$
CS	v_{CS}	independent	v_{TCA}
ACO2/IDH	$v_{ACO2/IDH}$	independent	v_{TCA}
GOT	v_{GOT}	dependent	$\frac{d_g}{1-d_g}v_{TCA}$
OGDC/SCS	$v_{OGDC/SCS}$	dependent	$\frac{d_g}{1-d_g}v_{TCA} + v_{TCA}$
SDH/Fh	$v_{GSDH/Fh}$	dependent	$\frac{d_g}{1-d_g}v_{TCA} + v_{TCA}$
MDH	v_{MDH}	dependent	$\frac{d_g}{1-d_g}v_{TCA} + v_{TCA} - v_{ME}$
PC	v_{PC}	dependent	$v_{TCA}\frac{d_a}{r}(1-r)$
ME	v_{ME}	independent	v_{ME}
PPCK	v_{PPCK}	independent	v_{PPCK}
AST	v_{AST}	dependent	$v_{TCA}\frac{d_a}{r}(1-r) - v_{ME} - v_{PPCK} + \frac{d_g}{1-d_g}v_{TCA}$
EXLAC	v_{EXLAC}	dependent	$\left(v_{TCA}\frac{d_a}{r} - v_{ME}\right)\frac{1}{d_l}$
EXFA	v_{EXFA}	dependent	$(1-d_a)v_{TCA}$
EXGLN	v_{EXGLN}	dependent	$v_{ME} + v_{PPCK} - v_{TCA}\frac{d_a}{r}(1-r)$
EXASP	v_{EXASP}	dependent	$v_{TCA}\frac{d_a}{r}(1-r) - v_{ME} - v_{PPCK} + \frac{d_g}{1-d_g}v_{TCA}$

Supplementary references

1. Wiechert, W. & Nöh, K. From Stationary to Instationary Metabolic Flux Analysis. in *Technology Transfer in Biotechnology: From lab to Industry to Production* (ed. Kragl, U.) 145–172 (Springer, 2005). doi:10.1007/b98921.
2. Nöh, K., Wahl, A. & Wiechert, W. Computational tools for isotopically instationary ¹³C labeling experiments under metabolic steady state conditions. *Metab. Eng.* **8**, 554–577 (2006).
3. Levenberg, K. A method for the solution of certain non-linear problems in least squares. *Q. Appl. Math.* **2**, 164–168 (1944).
4. Marquardt, D. W. An Algorithm for Least-Squares Estimation of Nonlinear Parameters. *J. Soc. Ind. Appl. Math.* **11**, 431–441 (1963).